INSTITUTE FOR ASTRONOMY
UNIVERSITY OF HAWAII
2680 WOODLAWN DRIVE
HONOLULU HAWAII 96822

FINAL REPORT

FOR

NATIONAL AERONAUTICS AND SPACE ADMINISTRATION

GRANT NAG 5-8216

FIP, FIT, OR MAD? ANALYSIS OF HIGH SIGNAL-to-NOISE ASCA SPECTRA OF CORONAL STARS

PRINCIPAL INVESTIGATOR: DR. THEODORE SIMON

For the period of
1999 FEBRUARY 15 - 2002 FEBRUARY 14

I. Major Scientific Goals of this Project

ASCA and EUVE spectra of active late-type stars imply that Fe and other medium-Z elements may be 2–10 times less abundant in the coronae of these stars than in their photo-spheres (the MAD effect). These deficiencies may be related to the solar FIP effect, in which Fe and other low First Ionization Potential elements appear enriched in the solar corona over their photospheric values. The FIP effect is time variable. As part of this proposal, the K0-2 III star, 29 Draconis, was observed in X rays with the ASCA spacecraft in order to measure the coronal abundances of this star at three different stellar longitudes over its 31-day rotation cycle. The goal of the observations was to learn whether coronal abundances, and hence coronal magnetic structure, vary across the surface of 29 Draconis in phase with the motion of dark star-spots across its disk. A second task included in this project was a systematic reanalysis of 18–20 deep exposures of active coronal stars, which were extracted from the ASCA public archives. New thermal models were computed for each spectrum in order to derive coronal metal abundances for each star. The goal of this survey was to search for possible trends in coronal abundance with various stellar parameters such as rotation, chromospheric activity levels at ultraviolet and optical wavelengths, or evolutionary stage, etc.

II. Final Status Report and Science Results

The observations of 29 Draconis were carried out successfully by ASCA. The three datasets obtained by ASCA were reduced using XSELECT and then modelled within XSPEC. The first two figures appended below illustrate the typical SIS and GIS extraction windows that were used to accumulate the X-ray counts, generate X-ray light curves, and measure the X ray spectra of this star, and also for measuring the datasets from the public archive that were examined in the course of this project. The following graph presents a plot of the SIS0 light curve obtained at one of the three stellar longitudes of 29 Draconis. In this instance, no strong short-term time variability is evident over the duration of the ASCA pointing. The following graph is a plot of the observed SIS0 spectrum, along with a best-fitting MEKAL thermal model, which provides for two separate temperature components, each having variable metal abundance. Based on the SIS0 specta alone, the abundances from each observation of 29 Draconis were inferred to be 5–6 times subsolar, with no significant differences in the model parameters as a function of stellar longitude. The close similarity of the results from the distinct datasets implies a relatively uniform arrangement of coronal structure and activity over the surface of this star. This is an unexpected finding, considering that starspots and hence chromospheric activity are very unevenly distributed over the different hemispheres of the star.

In subsequent study of this star, the two-temperature, variable-abundance MEKAL models were extended in order to attempt simultaneous fits to the spectra obtained by all four cameras aboard ASCA (SIS0, SIS1, GIS2, and GIS3). More complicated model fits also were tried. The results were not entirely satisfactory. For example, the next figure shows the results of a simultaneous XSPEC model fit to an observation of 29 Draconis that used the data from all four cameras. While the fit to the SIS0 and SIS1 spectra is acceptable, there is a systematic discrepancy in the lowest energy channels of the GIS2 and GIS3 spectra. This in turn was reflected in the very large uncertainties of the deduced model parameters, in particular for the metal abundances, and the unacceptably large reduced chi-squared value for this model. Under the assumption that part of the discrepancy might be due to temporal changes in the camera gains, additional models were run in which the gains of the cameras were treated as free parameters and then solved for as part of the model solution. This did not substantially improve the quality of the fits. More complicated VMEKAL models were tried in which the abundances of individual chemical elements were allowed to vary independently. As shown by the computer output on the following two pages, the results were quite poor, with most abundances being indeterminate.

ASCA exposures of various stars, including those listed in the table below in the original ADP proposal, were downloaded from the public archives, re-extracted, and then fitted with XSPEC thermal

models in a similar manner. In all, more than two dozen spectra were analyzed with multi-T component models having variable abundances. Other stars not listed in the table that were analyzed include 24 UMa, YZ CMi, σ CrB, ξ UMa, HR 5235, HR 764, and EI Eri. 2-T variable abundance MEKAL models (and in some cases, much more complicated models) were fitted to all of the spectra. As was the case for 29 Draconis, it was not possible to achieve a consistent fit with acceptable reduced chi-squared and acceptable errors on the model parameters to all four instruments (SIS0, SIS1, GIS2, and GIS3) simultaneously. As is illustrated by the last figure below, which shows the data and model fit for the star YY Men, the difficulty in finding overall agreement is not restricted to just one star, 29 Draconis, but almost certainly is connected to the systematic loss of sensitivity of the cameras at energies below E < 1 keV, where the detector response is known to have degraded appreciably with time (ASCA GOF Calibration Memo ASCA-CAL-00-06-01). It is expected that this issue will be addressed in building the final ASCA Data Archive, and while that effort has been considerably delayed, once it is completed it may be worth the effort to revisit the science goals of this project.

Dearchived ASCA Observations

	Star Name	ASCA Seq. No.	Expos (ks)	SIS CR (cts/s)
1	HD 32918	22011	25.5	1.18
2	HD 36705	21003	64.6	2.22
3	AU Mic	23046	30.8	1.10
4	TY Pyx	23034	69.7	0.90
5	β Ceti	21019	32.4	1.00
6	HD 35850	23026	35.6	0.63
7	ε Eri	22009	50.0	1.16
8	HR 1099	22017	75.4	8.44
9	FK Com	22032	27.8	1.00
10	II Peg	23027	79.9	1.38
11	UX Ari	22036	41.7	1.14
12	TZ CrB	22035	38.7	3.44
13	Algol	20024	130.	12.6
14	AR Lac	20023	151.	1.05
15	α Aur	20001	31.4	1.22
16	44 Boo	24044	126.	0.63
17	CH Cyg	42020	38.3	0.49
18	VW Cep	21011	39.5	0.44

file: dra02_s0.img
dir: /scr1/ASCA/29dra02

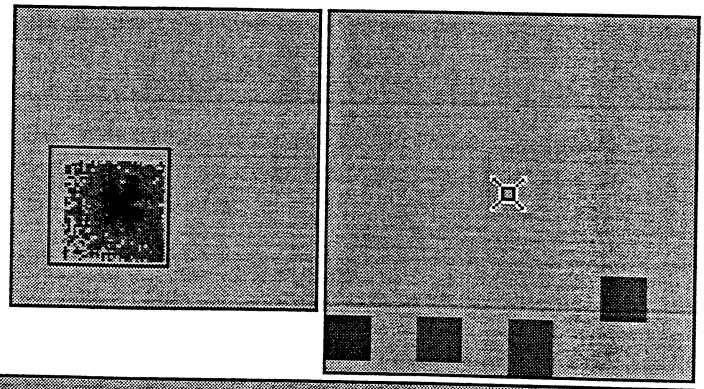

108.5 158.2 0

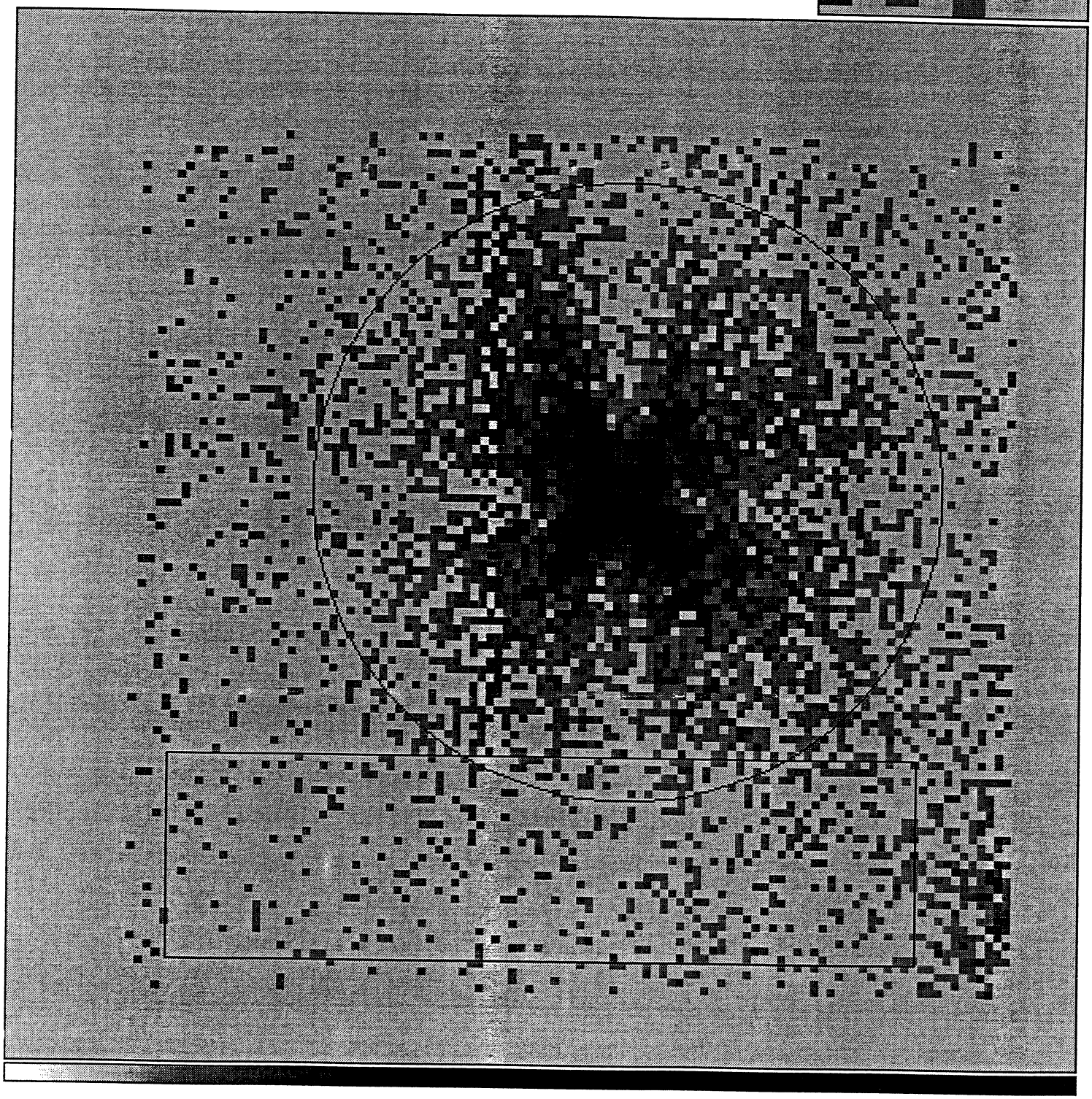

file: dra02_g2_image.xsl
dir: /scr1/ASCA/29dra02

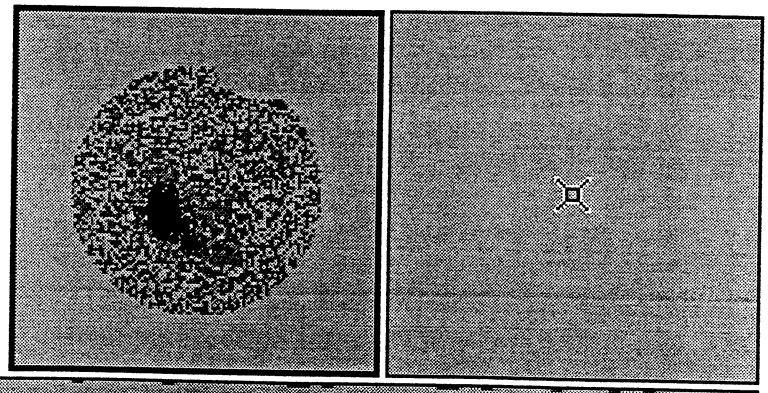

186.5 246.0 0

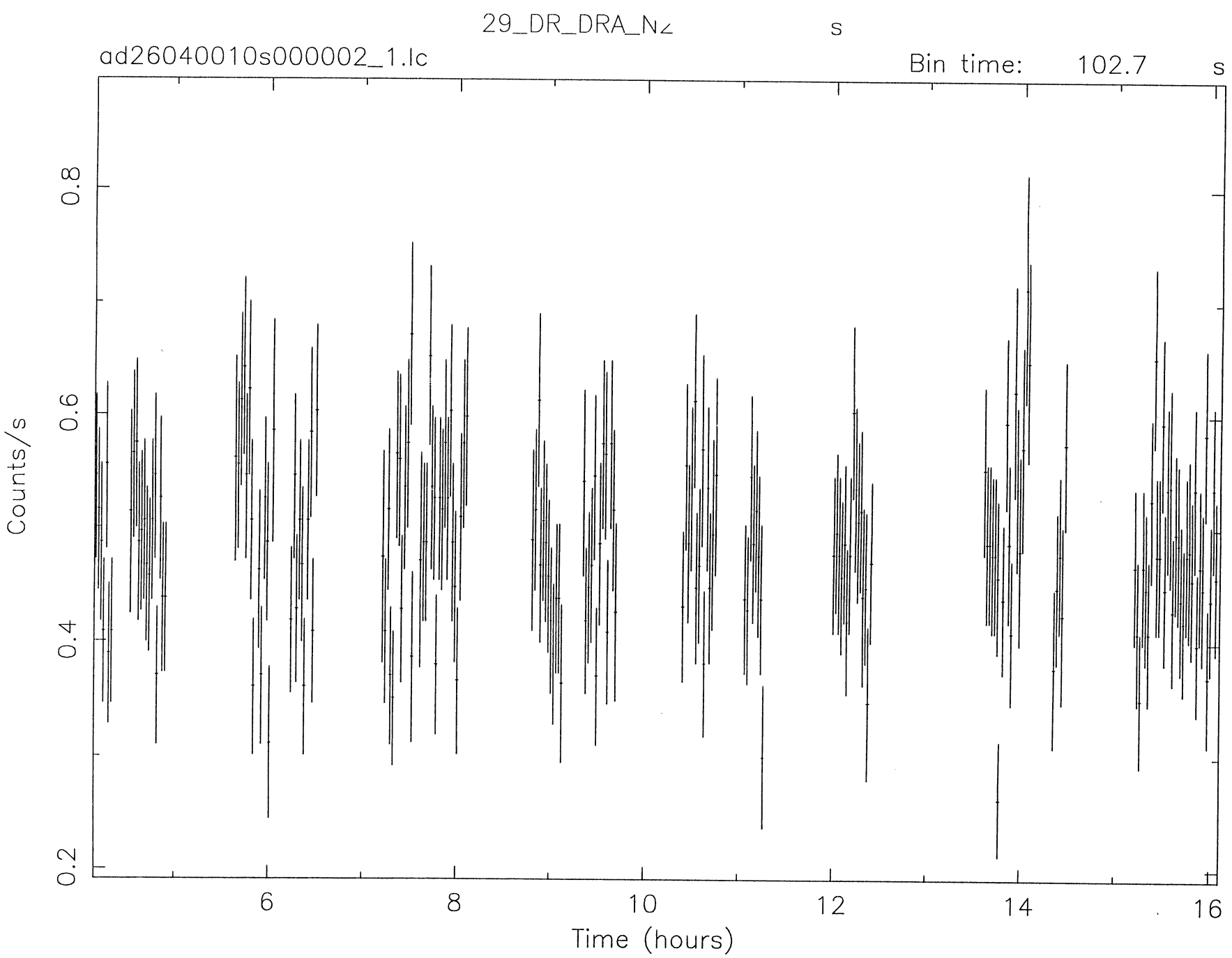

Start Time 10907 4: 9:34:463 Stop Time 10907 16: 3:32:848

9-May-1998 20:09

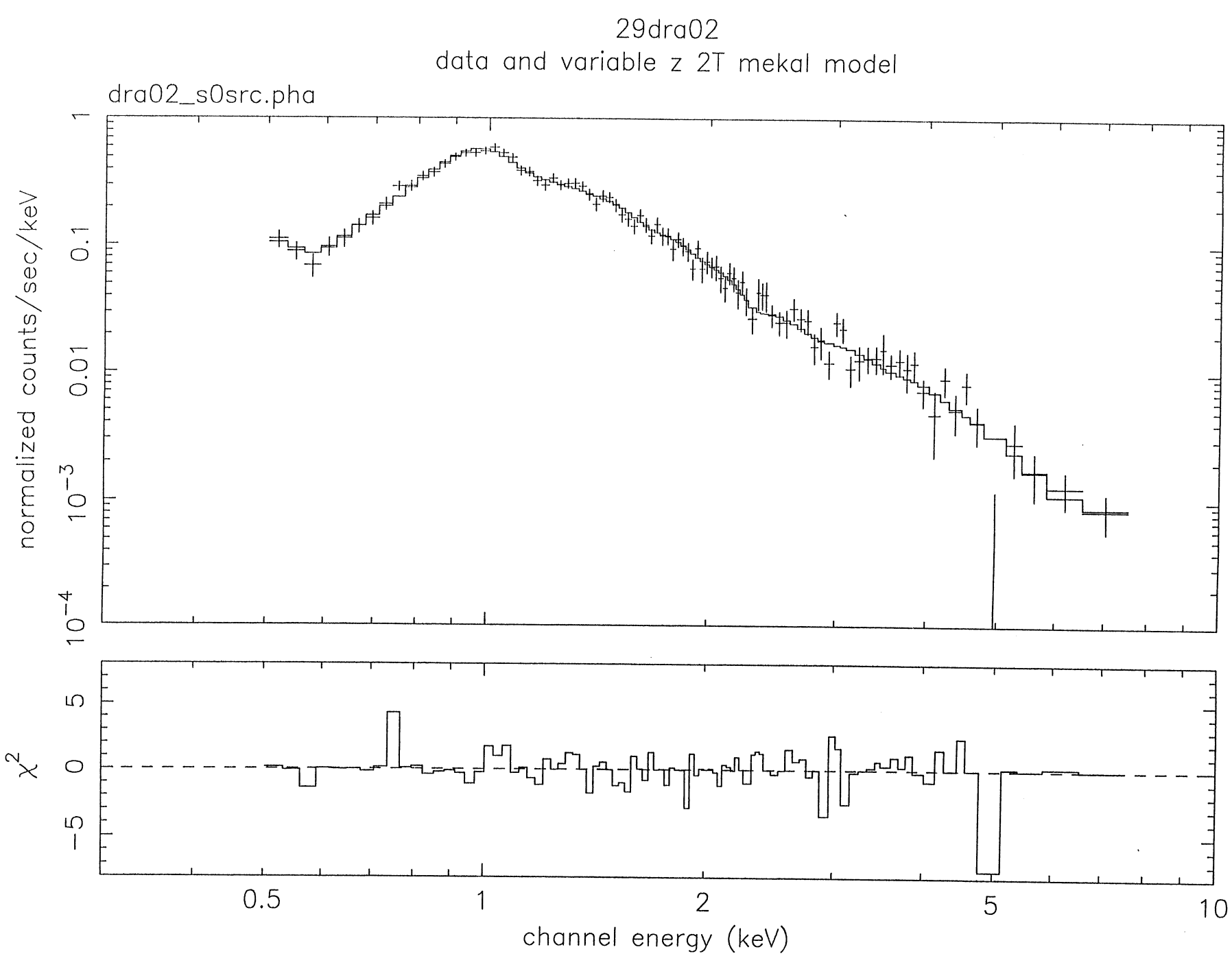

simon 24−May−1999 09:11

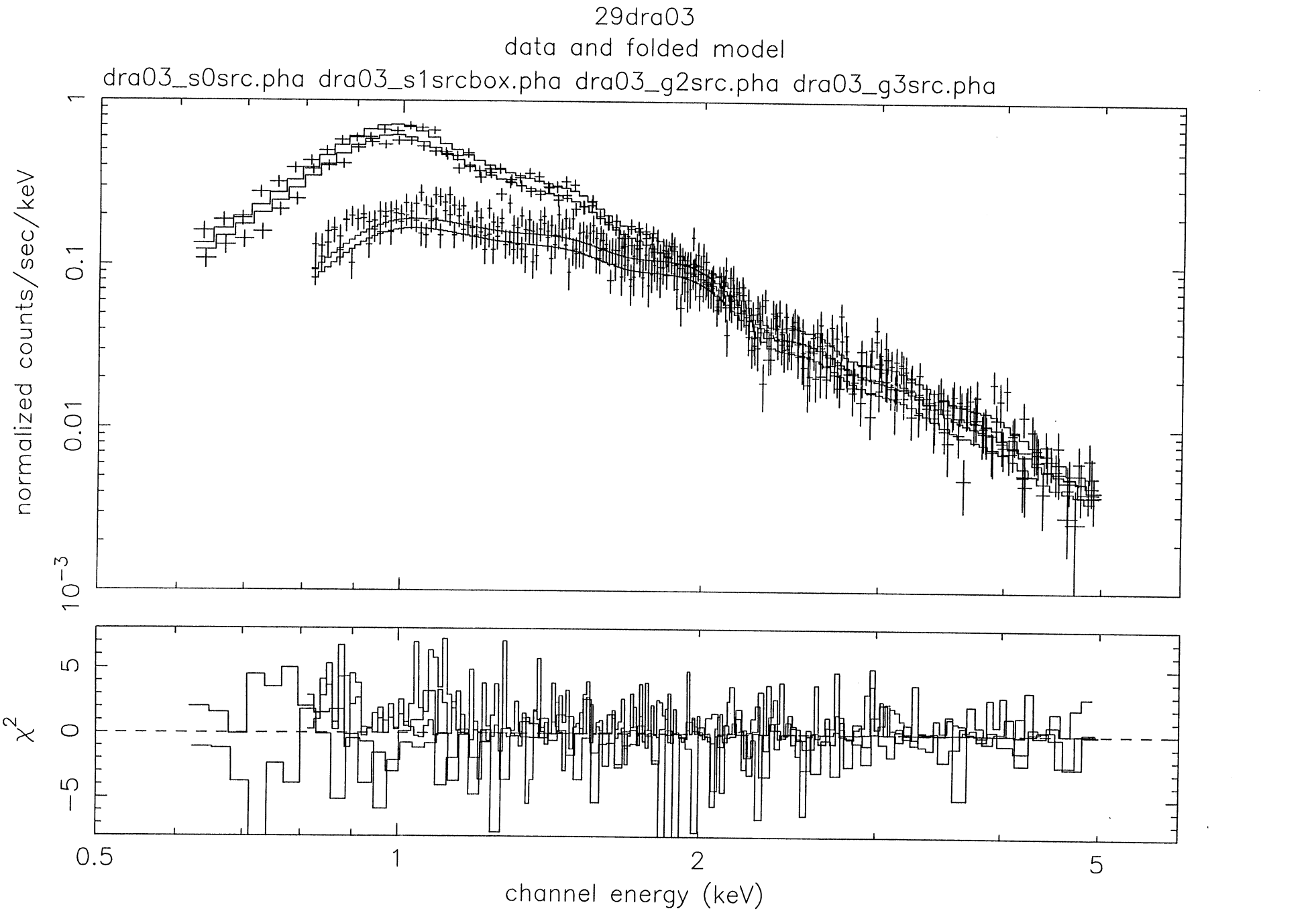

simon 8-Jun-1999 09:53

```
XSPEC> show all
 08:54:17 27-May-99
 Auto-saving is done after every command.
 Fit statistic in use is Chi-Squared
 Minimization technique is Lev-Marq
  Convergence criterion =      1.0000000000000D-02
 Querying enabled
 Prefit-renorming enabled
 Solar abundance table is angr

 Information for file   1
  belonging to plot group   1, data group   1
 telescope = ASCA , instrument = SIS0 , channel type = PI
  Current data file: dra01_s0src.pha
  Background file  :dra01_s0bakbox.pha
  No current correction
  Response (RMF) file     : dra01_s0.rmf
  Auxiliary (ARF) file     : dra01_s0.arf
  XSPEC filter : none
 Weighting method is standard
  Noticed channels    18 to   109
  File integration time     1.7613E+04
     and effective area      1.000
  File observed count rate     0.3812     +/-5.46494E-03 cts/s
  Model predicted rate :   0.4124

 Information for file   2
  belonging to plot group   2, data group   1
 telescope = ASCA , instrument = SIS1 , channel type = PI
  Current data file: dra01_s1src.pha
  Background file  :dra01_s1bakbox.pha
  No current correction
  Response (RMF) file     : dra01_s1.rmf
  Auxiliary (ARF) file     : dra01_s1.arf
  XSPEC filter : none
 Weighting method is standard
  Noticed channels    18 to   103
  File integration time     1.7713E+04
     and effective area      1.000
  File observed count rate     0.3215     +/-4.65250E-03 cts/s
  Model predicted rate :   0.3247

 Information for file   3
  belonging to plot group   3, data group   1
 telescope = ASCA , instrument = GIS2 , channel type = PI
  Current data file: dra01_g2src.pha
  Background file  :dra01_g2bak.pha
  No current correction
  Response (RMF) file     : /cdrom/26040000/26040000/spectra/gis2v4_0.rmf
  Auxiliary (ARF) file     : dra01_g2.arf
  XSPEC filter : none
 Weighting method is standard
  Noticed channels    70 to   204
  File integration time     2.1406E+04
     and effective area      1.000
  File observed count rate     0.1687     +/-3.02117E-03 cts/s
  Model predicted rate :   0.1522

 Information for file   4
  belonging to plot group   4, data group   1
 telescope = ASCA , instrument = GIS3 , channel type = PI
  Current data file: dra01_g3src.pha
  Background file  :dra01_g3bak.pha
  No current correction
  Response (RMF) file     : /cdrom/26040000/26040000/spectra/gis3v4_0.rmf
  Auxiliary (ARF) file     : dra01_g3.arf
```

```
 XSPEC filter : none
Weighting method is standard
 Noticed channels    70 to   214
 File integration time    2.1406E+04
    and effective area     1.000
 File observed count rate    0.1995    +/-3.24808E-03 cts/s
 Model predicted rate :   0.1760

 mo = wabs[1]( vmekal[2] + vmekal[3] )
------------------------------------------------------------------------
------------------------------------------------------------------------
 mo = wabs[1]( vmekal[2] + vmekal[3] )
 Model Fit Model Component  Parameter  Unit     Value
 par   par comp
   1     1    1   wabs       nH        10^22     7.6158E-02 +/-  0.2922E-01
   2     2    2   vmekal     kT        keV       0.8392     +/-  0.4758E-01
   3     3    2   vmekal     nH        cm-3       1.000     frozen
   4     4    2   vmekal     He                   1.000     frozen
   5     5    2   vmekal     C                    1.000     frozen
   6     6    2   vmekal     N                    1.000     frozen
   7     7    2   vmekal     O                   0.7155     +/-   5.248
   8     8    2   vmekal     Ne                  0.5396     +/-   5.301
   9     9    2   vmekal     Na                   1.000     frozen
  10    10    2   vmekal     Mg                   1.161     +/-   1.442
  11    11    2   vmekal     Al                   1.000     frozen
  12    12    2   vmekal     Si                  0.4920     +/-  0.5775
  13    13    2   vmekal     S                  2.5689E-25   +/-   1.129
  14    14    2   vmekal     Ar                   1.000     frozen
  15    15    2   vmekal     Ca                   1.000     frozen
  16    16    2   vmekal     Fe                  0.3365     +/-  0.3900
  17    17    2   vmekal     Ni                   1.000     frozen
  18    18    2   vmekal     Redshift               0.      frozen
  19    19    2   vmekal     Switch               1.000     frozen
  20    20    2   vmekal     norm               4.2098E-03   +/-  0.6483E-02
  21    21    3   vmekal     kT        keV        2.324     +/-  0.5786
  22    22    3   vmekal     nH        cm-3       1.000     frozen
  23    23    3   vmekal     He                   1.000     frozen
  24     5    3   vmekal     C                    1.000     = par   5
  25     6    3   vmekal     N                    1.000     = par   6
  26    27    3   vmekal     O                  8.0323E-15   +/-   21.10
  27    28    3   vmekal     Ne                 2.9386E-04   +/-   20.35
  28     9    3   vmekal     Na                   1.000     = par   9
  29    29    3   vmekal     Mg                 6.0460E-13   +/-   2.499
  30    11    3   vmekal     Al                   1.000     = par  11
  31    30    3   vmekal     Si                  0.6154     +/-  0.4214
  32    31    3   vmekal     S                   0.2019     +/-  0.3418
  33    14    3   vmekal     Ar                   1.000     = par  14
  34    15    3   vmekal     Ca                   1.000     = par  15
  35    32    3   vmekal     Fe                  0.5260     +/-  0.2348
  36    17    3   vmekal     Ni                   1.000     = par  17
  37    24    3   vmekal     Redshift               0.      frozen
  38    25    3   vmekal     Switch               1.000     frozen
  39    26    3   vmekal     norm               6.4415E-03   +/-  0.5441E-02
------------------------------------------------------------------------
------------------------------------------------------------------------
 Chi-Squared =      547.4473     using    458 PHA bins.
 Reduced chi-squared =      1.241377     for     441 degrees of freedom
 Null hypothesis probability = 4.001E-04
XSPEC> log none
```

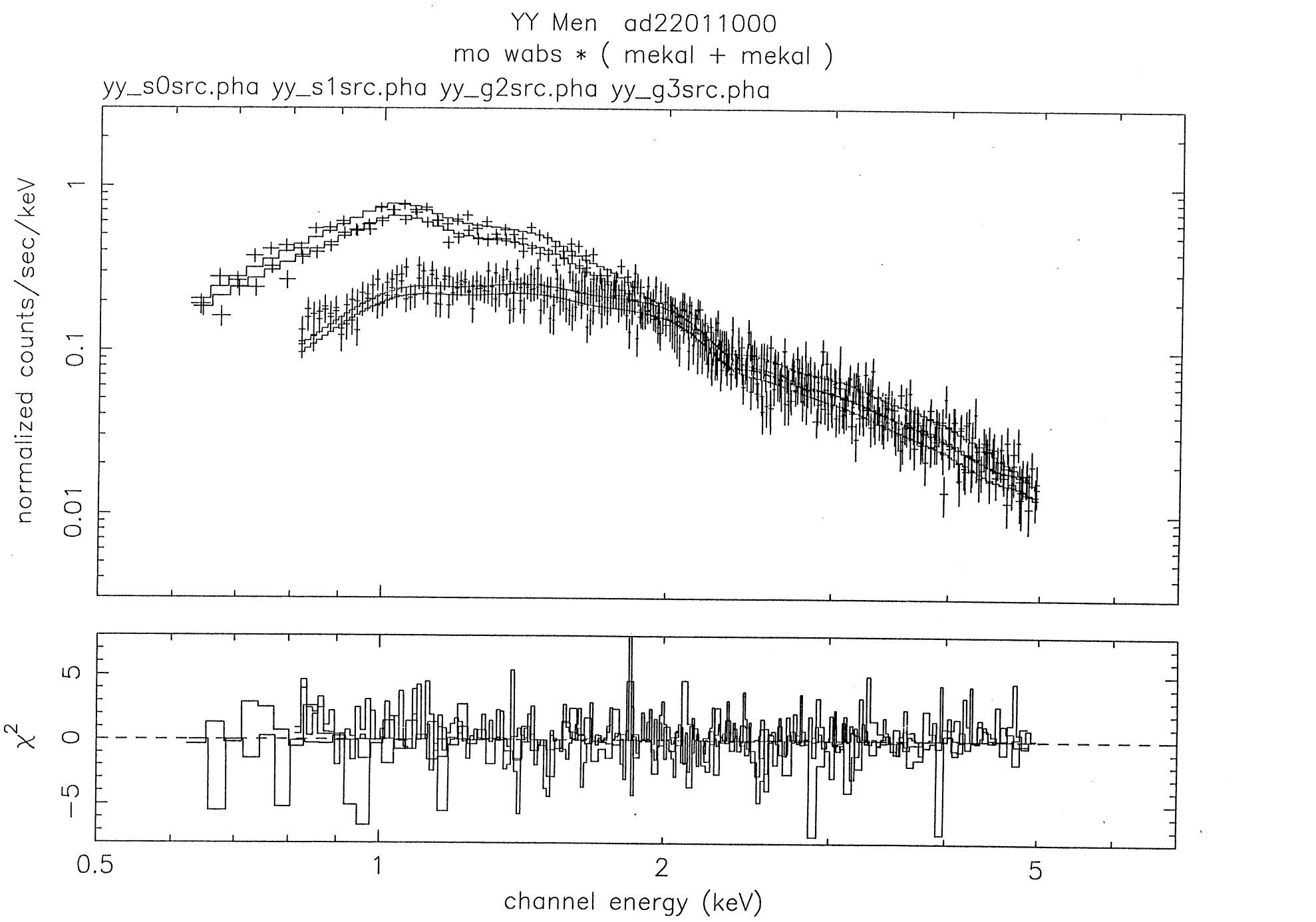

simon 29-Jun-1999 09:37